AFRL-VA-WP-TP-2006-303

ANTI-WINDUP CONTROL FOR AN AIR-BREATHING HYPERSONIC VEHICLE MODEL (PREPRINT)

Kevin P. Groves, Andrea Serrani, and Stephen Yurkovich
Michael A. Bolender and David B. Doman

DECEMBER 2005

Approved for public release; distribution is unlimited.

STINFO FINAL REPORT

AIR VEHICLES DIRECTORATE
AIR FORCE RESEARCH LABORATORY
AIR FORCE MATERIEL COMMAND
WRIGHT-PATTERSON AIR FORCE BASE, OH 45433-7542

NOTICE

PAO Case Number: AFRL/WS-06-0036, 4 Jan 2006.

THIS TECHNICAL REPORT IS APPROVED FOR PUBLICATION.

/s/

Michael A. Bolender
Aerospace Engineer
Control Design and Analysis Branch
Air Force Research Laboratory
Air Vehicles Directorate

/s/

Deborah S. Grismer
Chief
Control Design and Analysis Branch
Air Force Research Laboratory
Air Vehicles Directorate

/s/

Brian W. Van Vliet
Chief
Control Sciences Division
Air Force Research Laboratory
Air Vehicles Directorate

REPORT DOCUMENTATION PAGE			Form Approved OMB No. 0704-0188

1. REPORT DATE *(DD-MM-YY)*	2. REPORT TYPE	3. DATES COVERED *(From - To)*
December 2005	Conference Paper Preprint	12/01/2004 – 12/01/2005

4. TITLE AND SUBTITLE	
ANTI-WINDUP CONTROL FOR AN AIR-BREATHING HYPERSONIC VEHICLE MODEL (PREPRINT)	5a. CONTRACT NUMBER F33615-01-C-3154
	5b. GRANT NUMBER
	5c. PROGRAM ELEMENT NUMBER 0601102
6. AUTHOR(S) Kevin P. Groves, Andrea Serrani, and Stephen Yurkovich (The Ohio State University) Michael A. Bolender and David B. Doman (AFRL/VACA)	5d. PROJECT NUMBER A02D
	5e. TASK NUMBER
	5f. WORK UNIT NUMBER 0A
7. PERFORMING ORGANIZATION NAME(S) AND ADDRESS(ES) The Ohio State University Collaborative Center of Control Science Dept. of Electrical and Computer Engineering 2015 Neil Avenue. Suite 205 Columbus, OH 43210 Control Design and Analysis Branch (AFRL/VACA) Control Sciences Division, Air Vehicles Directorate Air Force Research Laboratory Air Force Materiel Command Wright-Patterson AFB, OH 45433-7542	8. PERFORMING ORGANIZATION REPORT NUMBER
9. SPONSORING/MONITORING AGENCY NAME(S) AND ADDRESS(ES) Air Vehicles Directorate Air Force Research Laboratory Air Force Materiel Command Wright-Patterson Air Force Base, OH 45433-7542	10. SPONSORING/MONITORING AGENCY ACRONYM(S) AFRL/VACA
	11. SPONSORING/MONITORING AGENCY REPORT NUMBER(S) AFRL-VA-WP-TP-2006-303

12. DISTRIBUTION/AVAILABILITY STATEMENT

Approved for public release; distribution is unlimited.

13. SUPPLEMENTARY NOTES

Conference paper preprint to be presented at the 2006 AIAA Guidance, Navigation, and Control Conference, 24 Aug 06, Keystone, CO. This report contains color.

This work has been submitted to AIAA for publication in the 2006 AIAA Guidance, Navigation, and Control Conference proceedings. One or more of the authors is a U.S. Government employee working within the scope of their position; therefore, the U.S. Government is joint owner of the work. If published, AIAA, Kevin P. Groves, Andrea Serrani, and/or Stephen Yurkovich may assert copyright. If so, the Government has the right to copy, distribute, and use the work. Any other form of use is subject to copyright restrictions.

14. ABSTRACT

An anti-windup controller modification is implemented in control system design for a model of the longitudinal dynamics of an air-breathing hypersonic vehicle. Anti-windup control allows the input constraints to be considered explicitly in the design of linear controllers to track a reference trajectory for the vehicle velocity, altitude, and angle of attack. The presence of anti-windup alleviates the need of keeping large penalties on the magnitude of the control input to avoid the occurrence of saturation. This, in turn, allows tighter tuning of the controller gains to obtain faster and more accurate trajectory tracking. The paper employs recent developments in anti-windup design to deal with the presence of exponentially unstable dynamics, which are typically encountered in air-breathing vehicle models. Simulation results on a fully nonlinear model are presented to validate the controller design.

15. SUBJECT TERMS Anti-windup, Control Theory, Flight Control, Hypersonic Aircraft

16. SECURITY CLASSIFICATION OF:			17. LIMITATION OF ABSTRACT:	18. NUMBER OF PAGES	19a. NAME OF RESPONSIBLE PERSON (Monitor)
a. REPORT	b. ABSTRACT	c. THIS PAGE			Michael A. Bolender
Unclassified	Unclassified	Unclassified	SAR	20	19b. TELEPHONE NUMBER *(Include Area Code)* (937) 255-8494

Standard Form 298 (Rev. 8-98)
Prescribed by ANSI Std. Z39-18

Anti-Windup Control for an Air-breathing Hypersonic Vehicle Model

Kevin P. Groves*
Andrea Serrani†
Stephen Yurkovich‡
Collaborative Center of Control Science
The Ohio State University, Columbus, OH 43210 USA

Michael A. Bolender§
David B. Doman¶
Air Force Research Laboratory, Wright-Patterson AFB, OH 45433

An anti-windup controller modification is implemented in control system design for a model of the longitudinal dynamics of an air-breathing hypersonic vehicle. Anti-windup control allows the input constraints to be considered explicitly in the design of linear controllers to track a reference trajectory for the vehicle velocity, altitude, and angle of attack. The presence of anti-windup alleviates the need of keeping large penalties on the magnitude of the control input to avoid the occurrence of saturation. This, in turn, allows tighter tuning of the controller gains to obtain faster and more accurate trajectory tracking. The paper employs recent developments in anti-windup design to deal with the presence of exponentially unstable dynamics, which are typically encountered in air-breathing vehicle models. Simulation results on a fully nonlinear model are presented to validate the controller design.

Keywords: anti-windup, tracking, hypersonic, air-breathing, control

I. Introduction

Seen as a possible way of making space access more affordable, air-breathing hypersonic vehicles (HSVs) have been studied sporadically over the last five decades as the technical advances necessary for their development were missing. New technology has brought a renewed interest in the research area, as demonstrated by the successful flights of NASA's X-43A in April and November of 2004. Air-breathing hypersonic vehicles are characterized by their unique design, incorporating a supersonic combustion ramjet engine located beneath the fuselage. This esoteric configuration results in strong coupling between the thrust and pitch dynamics of the vehicle, which in combination with flexible effects and static instability make the vehicle a challenging application for control. Control

*Control Engineer, Harris Corporation, FL.
†Assistant Professor, Department of Electrical and Computer Engineering, 2015 Neil Ave., Member AIAA
‡Professor, Department of Electrical and Computer Engineering, 2015 Neil Ave., Columbus, OH
§Aerospace Engineer, AFRL/VACA, 2210 Eighth St. Suite 21, Senior Member AIAA
¶Senior Aerospace Engineer, AFRL/VACA, 2210 Eighth St. Suite 21, Fellow AIAA

of air-breathing hypersonic vehicles is a difficult task because of the strong interaction between the airframe and the engine dynamics resulting in sizable couplings between thrust and pitch moment.[2,11] Furthermore, due to the vehicle length, relative slenderness, and light weight, the vehicle dynamics is characterized by the presence of flexible modes which interact with the aerodynamic forces and moments.

In the literature, models of the longitudinal dynamics of air-breathing hypersonic vehicles have been developed,[1,3,9,11,13] with a few concerted efforts to incorporate guidance and control.[4,6,12,18] In the cited references, mostly linearized models of the vehicle dynamics have been considered for control design, with the noticeable exception of Tournes et al.,[18] where nonlinear variable structure control has been adopted. On the other hand, for hypersonic vehicle models with conventional actuation and negligible flexibility, the use of nonlinear control system design methodologies is more common.[5,10,14,15] Like many real world systems, air-breathing hypersonic vehicles have input saturations which must be considered in control design. Hard constraints on the inputs can lead to performance degradation and even instability. Anti-windup control provides a method for resisting this performance degradation and helping to avoid the onset of instability. Several anti-windup control methods are discussed in.[7,8,16,17]

In our previous work,[6] a linear set-point tracking controller was developed for a particular model of the longitudinal dynamics of an air-breathing HSV as developed in Bolender and Doman.[2] In that work however, the constraints on the inputs were not directly taken into account. Instead, they were accounted for manually by tuning the gains to keep the inputs in their valid operating ranges. With an anti-windup controller the constraints on the inputs can be taken into consideration at the level of the controller design. In addition, by re-tuning the gains of the nominal controller and increasing the speed of the reference trajectories, we can elicit a faster response from the system. Anti-windup control will also provide some measure of robustness to the physical constraints on the inputs in terms of stability.

Designing an anti-windup controller for an air-breathing hypersonic vehicle is a difficult and challenging task, largely because the linearized model of the air-breathing HSV is unstable. Most anti-windup control methods only deal with stable plants with input saturation such as the methods discussed in.[8] Global stabilization of a system with input saturation is not possible for systems that are exponentially unstable even with anti-windup control. In the latter case, the role of anti-windup control is to enlarge the region of attraction for the equilibrium of the system with input saturation. The work by Teel[16] provides a method for dealing with exponentially unstable plants. In this paper, Teel's method is applied to a case study on linear controller design for a recently developed nonlinear model of the longitudinal dynamics of an air-breathing HSV. By means of computer simulations, it is shown that with a judicious selection of the gain parameters, Teel's anti-windup design is capable of enlarging the domain of stability achieved by baseline linear controllers, and significantly improving the performance of the closed-loop system in terms of speed and fidelity of response in tracking setpoint references trajectories.

The paper is organized as follows: In Section II, we provide some background on anti-windup design, and some details on the method proposed in[16] to deal with unstable plants. In Section III, we briefly introduce the model of the longitudinal dynamics of the air-breathing HSV under consideration, and preset the baseline linear controller employed in the case study. Then, we present the implementation and discuss the results achieved by the anti-windup modification in Section IV. Finally, we draw some conclusions in Section V.

II. Background

Controller windup occurs when the control actuators reach their physical limits or saturations. This results in a difference between the output of the nominal controller and the actual input to the

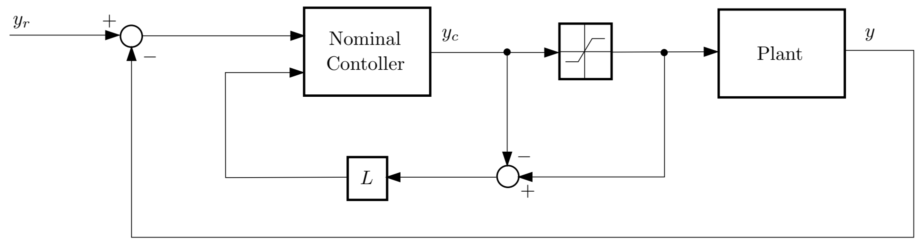

Figure 1. Block Diagram of Classical Anti-windup Modification

plant. Because of this difference the states of the system are incorrectly updated causing controller windup. Since the linear controller does not account for these input nonlinearities performance degradation, overshoot, and even instability can result. Many ad hoc methods have been developed over the years to modify pre-designed linear controllers to account for input saturation without local performance degradation. As mentioned previously, several of these methods are discussed in.[8] The majority of these methods require the plant to be stable, and are referred to as 'observer-based' or 'classical' anti-windup scheme. Consider a plant model given in the form

$$\begin{aligned} \dot{x}_p &= A_p x_p + B_p \mathrm{sat}(u_p) \\ y_p &= C_p x_p \end{aligned} \tag{1}$$

with state $x_p \in \mathbb{R}^n$ control input $u_p \in \mathbb{R}^m$, and regulated output $y_p \in \mathbb{R}^p$, endowed with a nominal controller given by the system

$$\begin{aligned} \dot{x}_c &= A_c x_c + B_c e_p \\ y_c &= C_c x_c + D_c e_p \end{aligned}$$

where $x_c \in \mathbb{R}^{n_c}, y_c \in \mathbb{R}^m$. The signal $e_p \in \mathbb{R}^p$ denotes the tracking error $e_p = y_r - y_p$, being y_r a reference trajectory. A vector-valued saturation nonlinearity of the form

$$\mathrm{sat}(u) = \begin{cases} \lambda_{\max} & \text{if } u \geq \lambda_{\max} \\ u & \text{if } \lambda_{\min} < u < \lambda_{\max} \\ \lambda_{\min} & \text{if } u \leq \lambda_{\min} \end{cases}$$

is present at the plant input, where the inequalities above are intended to hold componentwise, and $\lambda_{\max}$ and $\lambda_{\min}$ are vectors of upper and lower limits, respectively. We assume that under the interconnection $u_p = y_c$ the closed loop system without input constraints is well posed and internally stable.

The 'classical' anti-windup control method basically reduces to an output injection on the nominal controller. The nominal controller of the system is modified to be

$$\begin{aligned} \dot{x}_c &= A_c x_c + B_c e + L[\mathrm{sat}(u) - u] \\ u &= C_c x_c + D_c e\,. \end{aligned}$$

Figure 1 shows a block diagram of the observer-based scheme. Methods of this type are limited in their ability to control unstable systems: in deriving the error system between the constrained and unconstrained closed loop systems, it is readily seen that the eigenvalues of the plant matrix A_p are part of the set of eigenvalues for the error system. Thus if A_p has unstable eigenvalues, then the constrained closed loop system will diverge exponentially from its unconstrained counterpart when the inputs are saturated. The work by Teel and Kapoor[17] provides the basis for an anti-windup control method for unstable systems. In the cited reference, the authors provide the following definition of the anti-windup problem:

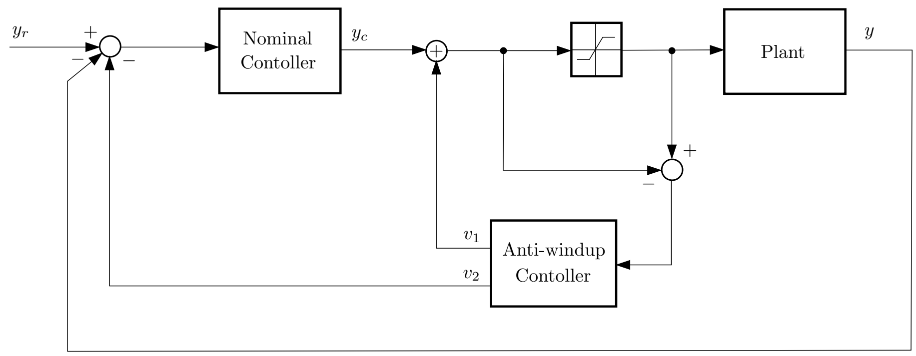

Figure 2. Block Diagram of Separate Anti-windup Controller Method

1. To have the closed loop system be unmodified in the absence of input saturation
2. To provide $\mathcal{L}_2$ stability for the error system created by the difference between the system with input constraints and the system without input constraints

The controller proposed in[17] modifies the closed loop system both at the input and the output to the nominal controller (see Figure 2). This anti-windup controller is given by

$$\begin{aligned} \dot{\xi} &= A_p\xi + B_p[\text{sat}(y_c+v_1) - y_c] \\ v_1 &= \kappa(\xi) \\ v_2 &= -C_p\xi \end{aligned} \tag{2}$$

where $\kappa(\xi)$ is a feedback term that stabilizes the error system (the mismatch between the constrained and unconstrained closed loop systems) in $\mathcal{L}_2$. The anti-windup controller changes the closed loop system by modifying the interconnections to $u_p = \text{sat}(y_c + v_1), u_c = y_p - y_r + v_2$. Though this is still an observer based solution, it creates n additional states giving enough degrees of freedom to blend the predesigned linear controller with a nonlinear anti-windup controller.

A. Teel's Method for Anti-Windup Design for Unstable Linear Systems

The problem of anti-windup for exponentially unstable linear systems is far more difficult than for stable systems. In unstable systems, once all inputs are saturated, the trajectories may grow unbounded. The goal of anti-windup control for unstable systems is to enlarge the domain of attraction of the equilibrium. The paper by Teel[16] illustrates these difficulties and derives a solution. This method takes the anti-windup solution given by Teel and Kapoor[17] and modifies it to account for the unstable modes. To this end, the system must first be transformed by separating the unstable modes from the stable ones such that the system can be given in the form

$$\begin{aligned} \begin{pmatrix} \dot{x}_\star \\ \dot{x}_+ \end{pmatrix} &= \begin{pmatrix} A_\star & A_{12} \\ 0 & A_+ \end{pmatrix} \begin{pmatrix} x_\star \\ x_+ \end{pmatrix} + \begin{pmatrix} B_\star \\ B_+ \end{pmatrix} \text{sat}(u) \\ y &= Cx \end{aligned} \tag{3}$$

where $x_\star$ and x_+ represent the states associated with the stable and unstable modes of the system respectively. Letting $x = (x_\star \; x_+)^T$, the system (3) is written as

$$\begin{aligned} \dot{x} &= Ax + B\text{sat}(u) \\ y &= Cx \end{aligned} \tag{4}$$

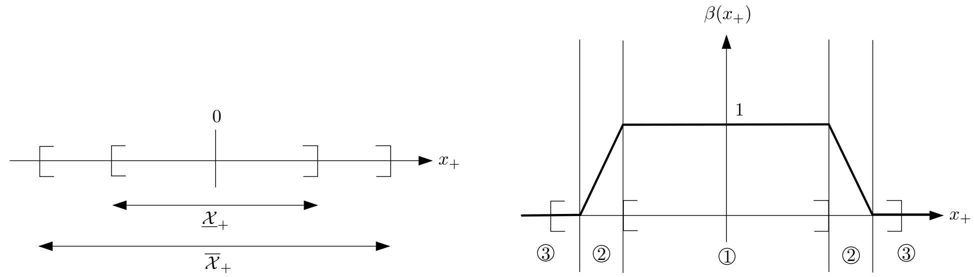

Figure 3. Region of Attraction for the Unstable Mode and Operating Region for $\beta(x_+)$

where $A = T^{-1}A_pT$, $B = T^{-1}B_p$, and $C = C_pT$. The solution of the anti-windup problem for exponentially unstable systems proposed by Teel employs a controller of the form

$$\begin{aligned} \dot{\xi} &= A\xi + B[\text{sat}(y_c + v_1) - y_c] \\ v_1 &= [\beta - 1]y_c + \alpha(x_+ - \beta[x_+ - \xi_+], \beta\kappa(\xi)) \\ v_2 &= -C\xi - D[\text{sat}(y_c + v_1) - y_c] \end{aligned} \tag{5}$$

where $\beta(x_+)$ is a function of $x_+(t)$ that takes values between zero and one, and $\kappa(\xi)$ is a feedback that provides $\mathcal{L}_2$ stability of the error system governing the mismatch between the constrained and unconstrained closed loop systems. The proof is given in,[16] and will obviously be omitted here; however, to understand the controller behavior, it is necessary to introduce some additional notation. Let $\overline{\mathcal{X}}_+$ be defined as the region of the state space in which $x_+(t)$, the state corresponding to the unstable mode, can be driven back to the origin, and let the set $\underline{\mathcal{X}}_+$ be conservatively chosen to be contained in $\overline{\mathcal{X}}_+$ (see Figure 3). The anti-windup controller given by equation (5) is divided into two separate controllers that span three different operating regions defined by the function $\beta(x_+)$ as shown in Figure 3. The function $\beta(x_+)$ is a design parameter, whose choice affects the performance of the anti-windup controller. When $x_+ \in \underline{\mathcal{X}}_+$ then $\beta(x_+) = 1$. When x_+ leaves $\underline{\mathcal{X}}_+$, then $\beta(x_+)$ linearly tapers off until it reaches zero. In general the function $\beta(x_+)$ can be chosen to be a piecewise linear function interpolated and extrapolated from chosen data points. These data points are related to the regions $\underline{\mathcal{X}}_+$ and $\overline{\mathcal{X}}_+$. In the first operating region ($x_+(t) \in \underline{\mathcal{X}}_+$, $\beta(x_+) = 1$), the anti-windup controller takes a form similar to the one given by equation (2) written as

$$\begin{aligned} \dot{\xi} &= A\xi + B[\text{sat}(y_c + v_1) - y_c] \\ v_1 &= \alpha(\xi_+, \kappa(\xi)) \\ v_2 &= -C\xi - D[\text{sat}(y_c + v_1) - y_c]. \end{aligned}$$

This will be referred to as the nominal anti-windup controller, and it can be designed in a similar manner as the anti-windup controller for stable systems presented in.[17] The function $\alpha(\xi_+, \kappa(\xi))$ can be chosen as

$$\alpha(\xi_+, \kappa(\xi)) = k_{1_e}\xi_+ + \kappa(\xi).$$

The feedback gain k_{1_e} is designed to make $A_+ + B_+k_{1_e}$ Hurwitz using LQR. Weighting is specifically placed on the unstable state to keep the trajectory bounded. We can then take the function $\kappa(\xi)$ to be the linear function $\kappa(\xi) = -B^TP\xi = -k_{2_e}\xi$. The feedback gain k_{2_e} is computed optimally using LQR methodology. This guarantees $\mathcal{L}_2$ stability of the error system as long as $x_+(t) \in \underline{\mathcal{X}}_+$.

The system response may require that $x_+(t)$ leaves the region $\underline{\mathcal{X}}_+$. In this case, the controller enters the second operating region, and the anti-windup controller takes the form given by equation (5). In this transitionary regime, both the nominal anti-windup controller and an auxiliary

anti-windup controller are active, with $\beta(x_+)$ determining the contribution from each controller. The auxiliary anti-windup control serves the purpose of keeping $x_+(t) \in \overline{\mathcal{X}}_+$ so that $\mathcal{L}_2$ stability is maintained and has the form

$$
\begin{aligned}
\dot{\xi} &= A\xi + B[\mathrm{sat}(y_c + v_1) - y_c] \\
v_1 &= -y_c + \alpha(x_+, 0) \\
v_2 &= -C\xi - D[\mathrm{sat}(y_c + v_1) - y_c].
\end{aligned}
$$

In the third operating region, the auxiliary anti-windup controller takes over and the nominal anti-windup controller is turned off. If x_+ goes outside of $\overline{\mathcal{X}}_+$ the trajectories will grow without bound since the unstable state will not be able to be driven back to the origin using the constrained input. Thus the goal of the auxiliary anti-windup controller is to keep $x_+ \in \overline{\mathcal{X}}_+$ and drive the state x_+ back into the region $\underline{\mathcal{X}}_+$. Obviously, anytime the auxiliary anti-windup controller is used, the response of the system will be altered more than for the nominal anti-windup controller. This is because the goal of the overall control scheme has shifted from trying to track the reference input, to trying to keep the unstable state from diverging. In this case, the reference trajectory which is commanded is not achievable using the constrained control inputs, so the system response deviates from the reference trajectory.

III. Anti-windup Implementation for Air-breathing HSVs

The longitudinal dynamics for the air-breathing hypersonic vehicle model considered in this paper, as given in Bolender and Doman,[2] is described by the following nonlinear equations

$$
\begin{aligned}
\dot{V}_t &= \frac{1}{m}\left(\mathcal{T}\cos\alpha - D\right) - g\sin(\theta - \alpha) \\
\dot{\alpha} &= \frac{1}{mV_t}\left(-\mathcal{T}\sin\alpha - L\right) + Q + \frac{g}{V_t}\cos(\theta - \alpha) \\
I_{yy}\dot{Q} &= M + \widetilde{\psi}_1\ddot{\eta}_1 + \widetilde{\psi}_2\ddot{\eta}_2 \\
\dot{h} &= V_t\sin(\theta - \alpha) \\
\dot{\theta} &= Q \\
k_1\ddot{\eta}_1 &= -2\zeta_1\omega_1\dot{\eta}_1 - \omega_1^2\eta_1 + N_1 - \widetilde{\psi}_1\frac{M}{I_{yy}} - \frac{\widetilde{\psi}_2\widetilde{\psi}_1\ddot{\eta}_1}{I_{yy}} \\
k_2\ddot{\eta}_2 &= -2\zeta_2\omega_2\dot{\eta}_2 - \omega_2^2\eta_2 + N_2 - \widetilde{\psi}_2\frac{M}{I_{yy}} - \frac{\widetilde{\psi}_1\widetilde{\psi}_2\ddot{\eta}_2}{I_{yy}},
\end{aligned}
$$

where $\mathcal{T}, L, D, N_i$ are the thrust, lift, drag, and generalized elastic forces respectively, M is the pitching moment about the y-axis, I_{yy} is the moment of inertia, ζ_i, ω_i are the damping coefficients and natural frequencies of the elastic modes. Furthermore,

$$
k_i = 1 + \frac{\widetilde{\psi}_i}{I_{yy}}, \quad i = 1,2 \qquad \widetilde{\psi}_1 = \int_{-L_f}^{0} \hat{m}_f\xi\phi_f(\xi)d\xi \qquad \widetilde{\psi}_2 = \int_{0}^{L_a} \hat{m}_a\xi\phi_a(\xi)d\xi\,,
$$

where $\hat{m}_f$, $\hat{m}_a$ are the mass densities of the forebody and aftbody respectively and ϕ_f, ϕ_a are the mode shapes for the forebody and aftbody respectively. The reader is referred to Bolender and Doman[2] for further details.

A linearized model about a trim condition of the nonlinear vehicle dynamics described by the equations above is given in the form (1), where $x_p \in \mathbb{R}^9$, $u_p \in \mathbb{R}^3$, and $y_p \in \mathbb{R}^3$ represent deviations

	States		Control Inputs
V_t	Vehicle velocity	δ_e	Control surface deflection
α	Angle-of-attack	ΔT_0	Total temperature change across combustor
Q	Pitch rate	A_d	Diffuser area ratio
h	Altitude		**Controlled Outputs**
θ	Pitch angle	V_t	Vehicle velocity
η_i	Generalized elastic coordinates	α	Angle-of-attack
$\dot{\eta}_i$	Time derivative of the elastic coordinates	h	Altitude

Table 1. Definitions of the states and inputs

States		Inputs	
V_t [ft/s]	7846.4	δ [rad]	0.13716
α [rad]	0.034217	ΔT_0 [deg R]	484.49
Q [rad/s]	0	A_d	0.35005
h [ft]	85000		
θ [rad]	0.034217		
η_1	1.6105		
η_2	1.4582		
$\dot{\eta}_i$	0		

Table 2. Trim condition

of the corresponding trajectories of the non-linear system from the trim condition. States, inputs and outputs are arranged in the same order as they are given in Table 1, while the trim condition is given in Table 2. The final performance objective is to achieve a simultaneous setpoint tracking of the angle of attack (α), velocity (V_t), and altitude (h) without the actuators violating specific constraints, given in Table 3. The plant has been augmented with integrators to remove the presence of steady-state error in setpoint tracking. After integral augmentation, the model is written as in (4). The nominal controller, based on the synthesis given in,[6] is a linear optimal tracking controller that minimizes the cost function

$$J = \frac{1}{2} \int_0^\infty \left(e^T Q e + u^T R u \right) dt,$$

where $Q = Q^T \geq 0$ and $R = R^T > 0$, subject to the *unconstrained* dynamics (4).

The nominal controller is then augmented with the nonlinear anti-windup scheme described in the previous section. As discussed in the previous section, optimal control techniques can also be used to calculate the gains k_{1_e} and k_{2_e}. Specifically, the cost function

$$J = \frac{1}{2} \int_0^\infty \left(\xi_+^T Q_+ \xi_+ + u^T u \right) dt$$

is employed to optimally determine the gain k_{1_e}, while the gain k_{2_e} is calculated using the cost function

$$J = \frac{1}{2} \int_0^\infty \left(\xi^T Q_\star \xi + u^T u \right) dt.$$

Input	Lower Limit	Upper Limit
δ [rad]	0.037369	0.3117
ΔT_0 [deg R]	34.495	2984.5
A_d	0.10005	1

Table 3. Input Constraints

The tuning of the weighting matrices for both optimization routines is discussed in the case study section. The choice of $\beta(x_+)$ for the air-breathing hypersonic vehicle is motivated by the behavior of x_+. Unfortunately, because we have multiple inputs, the explicit calculation of the region $\overline{\mathcal{X}}_+$ is very difficult. However, unless the unstable state reaches a value which causes it to grow without bound, the values of $\beta(x_+)$ can be set arbitrarily by choosing $\underline{\mathcal{X}}_+$. If $\underline{\mathcal{X}}_+$ is set too small it may result in performance degradation of the closed loop system. In the case of the air-breathing HSV model, the unstable state does not exceed $\overline{\mathcal{X}}_+$ for all the reference trajectories that are considered. Thus, simply setting the value of $\beta(x_+)$ to be large enough not to interfere with the system response is sufficient to achieve the desired response. The nominal anti-windup controller keeps x_+ inside $\underline{\mathcal{X}}_+$. The function $\beta(x_+)$ is chosen to be interpolated from the data points $\beta(-120) = 0$, $\beta(-110) = 0$, $\beta(-100) = 1$, $\beta(100) = 1$, $\beta(110) = 0$, $\beta(120) = 0$. Figure 4 shows the Simulink implementation of the closed loop system with anti-windup control. Notice that the scheme in Figure 4 is consistent with the one in Figure 2.

IV. Case Study of Anti-Windup Control for Air-breathing HSVs

In this section, the effectiveness of the anti-windup scheme will be shown by means of simulation. It will be demonstrated that, by means of a proper tuning of the weighting matrices, the problems posed by input saturation can be overcome at least locally. The tuning of the weighting matrices used for this case study are $Q_+ = 1$ and $Q_\star = 10^{-7} I_{9\times 9}$, which were determined iteratively to give favorable results. As discussed in,[6] the performance objective is to let angle-of-attack, velocity, and altitude to track step inputs filtered by three decoupled 2$^{\text{nd}}$ order command shaping filters. The filtered step inputs give a 1 degree command change in angle-of-attack, 1000 ft/s increase in velocity, and 10000 ft change in altitude, respectively. In this study, the constraints on the inputs are explicitly taken into account by the means of anti-windup control. Though the input constraints in Table 3 were chosen perhaps a little conservatively, only the diffuser area ratio A_d could really cause a problem. The diffuser area ratio can not be allowed to go too close to zero because this would choke the flow of air through the engine, causing the engine to shut down. Thus a lower limit of 0.1 was chosen to give the engine some breathing room.

1. First Case: Comparison to Nominal Linear Controller

In this first case, the effect of the anti-windup controller is illustrated using the same reference trajectories and nominal controller gains given in.[6] The reference trajectories have settling times of 3.6 [s] for α, 166 [s] for V_T, and 117 [s] for h. This case provides a basis of comparison for the controller with and without anti-windup compensation and input saturation. Figure 5(a) shows the system response on the nonlinear model in the absence of input constraints. This is the same response as given in [6] for the set-point tracking controller. Figure 5(c) shows the nonlinear system response with the input constraints taken into consideration. Notice that the response of the system with input constraints is worse than the response of the system without input constraints,

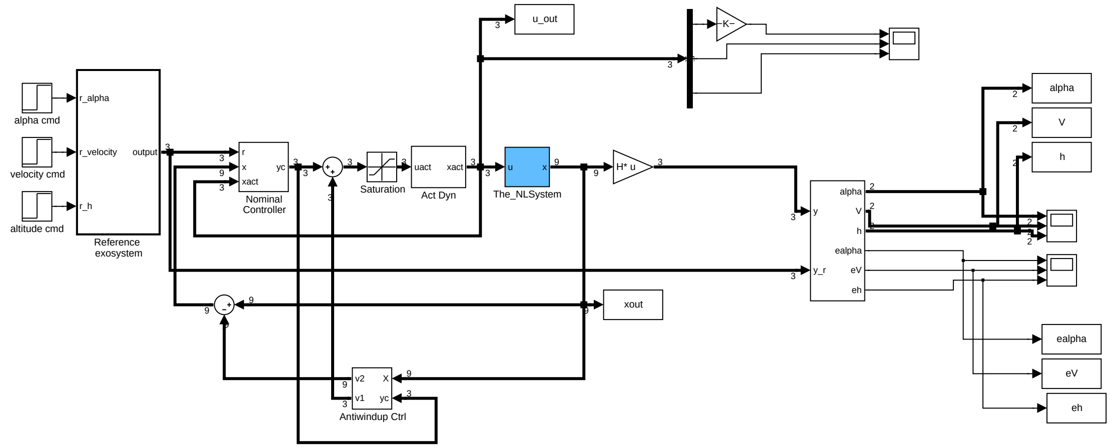

Figure 4. Simulink Block Diagram of Nonlinear System with Nominal and Anti-windup Control

particularly for the output $V_t(t)$. It is clear from Figure 5(d) the the inputs do indeed saturate, which leads to performance degradation. The effectiveness of anti-windup control becomes clear in Figure 5(e). The output response closely matches the system response without input constraints shown in Figure 5(a).

2. Second Case: Different Nominal Controller Gains

This example is useful in illustrating the advantages of using the anti-windup control method. Though the reference trajectories are still the same, the nominal controller gains have been adjusted to achieve tighter tracking of the reference trajectory as shown in Figure 6(a). As a result, in the absence of input constraints, the values of the inputs exceed their physical limitations. Figure 6(a) shows the response of the linearized system without constraints on the inputs. Figure 6(c) shows that with the input constraints, the system becomes unstable as soon as all three inputs simultaneously hit their saturations. The simulations for the system without anti-windup are performed on the linearized system, because the nonlinear simulation diverges rather quickly. The main advantage of anti-windup control is clear. In Figure 6(c) we see an unstable response when input constraints are included in the system. In Figure 6(e) we see that the anti-windup control has stabilized the system. In fact the system response is very close to the response in the absence of input constraints, as seen in Figure 6(a).

3. Third Case: Fast Reference Trajectories

One of the advantages that can be gained through anti-windup control is the ability to increase the speed of the reference trajectories. This set of reference trajectories have desirable properties because of their physically achievable and desirable settling times as discussed in.[6] Simple G-force calculations show that a desirable response should have a settling time of approximately 1.3 [s] for α, 102 [s] for V_T, and 60 [s] for h. Figures 7(a) and 7(b) show the linearized system response to the reference trajectories assuming that there is no saturation in the system, allowing the inputs to violate their constraints. The nonlinear simulation will not run in this case because this is not a physically realizable response. Figures 7(c) and 7(d) show the linearized system response when the input saturation is included, but the linear controller is not modified to include anti-windup control. It is clear from these graphs that the response with input saturation and without anti-windup control is unstable. Again this leads to a physically impossible situation, so the nonlinear

simulation will not run. When anti-windup control is included the system is stabilized even with the constraints on the system. Figure 7(e) is especially encouraging, because it comes close to matching the settling times of the reference trajectories with minimal overshoot.

V. Conclusions

This study has shown that anti-windup redesign is a viable solution to the problem of mitigating the effect of input saturation in tracking control of exponentially unstable systems, such as the model of air-breathing HSV under investigation. By means of trial-and-error iterations a good selection for the controller weights can be found, so that stable tracking is achieved. Anti-windup redesign has the potential to allow the controller to achieve faster output responses with respect to the case in which the constraints are implicitly accounted for by limiting the closed-loop bandwidth, resulting in increased transient performance and more robust asymptotic tracking.

Acknowledgments

This work was performed while the first author was a DAGSI Fellow at the Department of Electrical and Computer Engineering, The Ohio State University. The support of DAGSI and the AFRL/AFOSR Collaborative Center of Control Science at The Ohio State University under Grant no. F33615-01-2-3154 is gratefully acknowledged.

References

[1]K. D. Bilimoria and D. K. Schmidt. Integrated development of the equations of motion for elastic hypersonic flight vehicles. *Journal of Guidance, Control, and Dynamics*, 18(1):73–81, 1995.

[2]M. A. Bolender and D. B. Doman. A non-linear model for the longitudinal dynamics of a hypersonic air-breathing vehicle. Technical report, WPAFB/ARFL, 2004.

[3]F. R. Chavez and D. K. Schmidt. Analytical aeropropulsive/aeroelastic hypersonic-vehicle model with dynamic analysis. *Journal of Guidance, Control, and Dynamics*, 17(6):1308–1319, 1994.

[4]J. Davidson, F. Lallman, J. D. McMinn, J. Martin, J. Pahle, M. Stephenson, J. Selmon, and D. Bose. Flight control laws for NASA's hyper-x research vehicle. In *Proceedings of AIAA Guidance, Navigation, and Control Conference and Exhibit*, number AIAA-1999-4124, Portland, OR, 1999.

[5]D. B. Doman and A. D. Ngo. Dynamic inversion-based adaptive/reconfigurable control of the x-33 on ascent. *Journal of Guidance, Control, and Dynamics*, 25(2):275–84, 2002.

[6]K. P. Groves, D. O. Sigthorsson, A. Serrani, S. Yurkovich, M. A. Bolender, and D. B. Doman. Reference command tracking for a linearized model of an air-breathing hypersonic vehicle. In *Proceedings of AIAA Guidance, Navigation, and Control Conference*, number AIAA-2005-6144, San Francisco, CA, USA, 2005.

[7]N. Kapoor, A. .R. Teel, and P. Daoutidis. An anti-windup design for linear systems with input saturation. *Automatica*, 34(5):559–574, 1998.

[8]M. V. Kothare, P. J. Campo, M. Morari, and C. N. Nett. A unified framework for the study of anti-windup designs. *Automatica*, 30:1869–1883, 1994.

[9]D. McRuer. Design and modelling issues for integrated airframe/propulsion control of hypersonic flight vehicles. In *Proceedings of the American Control Conference*, pages 729–734, Boston, MA, 1992.

[10]M. D. Mirmirani, H. Xu, and P. A. Ioannou. Adaptive sliding mode control design for a hypersonic flight vehicle. *Journal of Guidance, Control, and Dynamics*, 27(5):829–838, 2004.

[11]D. K. Schmidt. Dynamics and control of hypersonic aeropropulsive/aeroelastic vehicles. *AIAA Paper*, AIAA-92-4326, 1992.

[12]D. K. Schmidt. Optimum mission performance and multivariable flight guidance for air-breathing launch vehicles. *Journal of Guidance, Control, and Dynamics*, 20(6):1157–64, 1997. Nonlinear Dynamical Systems.

[13]D. K. Schmidt and J. R. Velapoldi. Flight dynamics and feedback guidance issues for hypersonic air-breathing vehicles. In *Proceedings of AIAA Guidance, Navigation, and Control Conference and Exhibit*, number AIAA-1999-4122, pages 859–871, Portland, OR, 1999.

[14]R. F. Stengler and C. I. Marrison. Design of robust control systems for a hypersonic aircraft. *Journal of Guidance, Control, and Dynamics*, 21(1):58–63, 1998.

[15]R. F. Stengler and Q. Wang. Robust control systems for a hypersonic aircraft. *Journal of Guidance, Control, and Dynamics*, 23(4):577–588, 2000.

[16]A. R. Teel. Anti-windup for exponentially unstable linear systems. *International Journal of Robust and Nonlinear Control*, 9:701–716, 1999.

[17]A. R. Teel and N. Kapoor. The $\mathcal{L}_2$ anti-windup problem: Its definition and solution. In *Proceedings of the European Control Conference*, Brussels, Belgium, 1997.

[18]C. Tournes, D. B. Landrum, Y. Shtessel, and C. W. Hawk. Ramjet-powered reusable launch vehicle control by sliding modes. *Journal of Guidance, Control, and Dynamics*, 21(3):409–15, 1998.

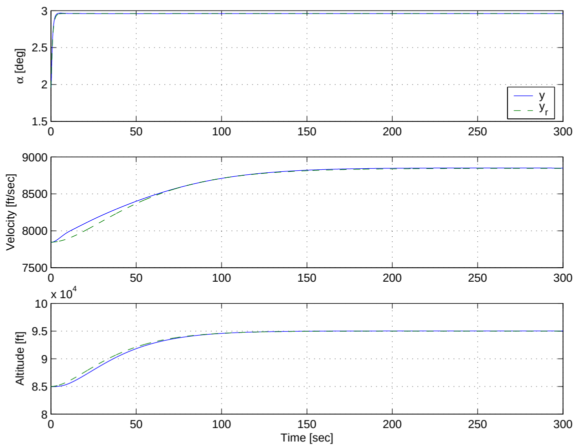

(a) Outputs with no Input Constraints

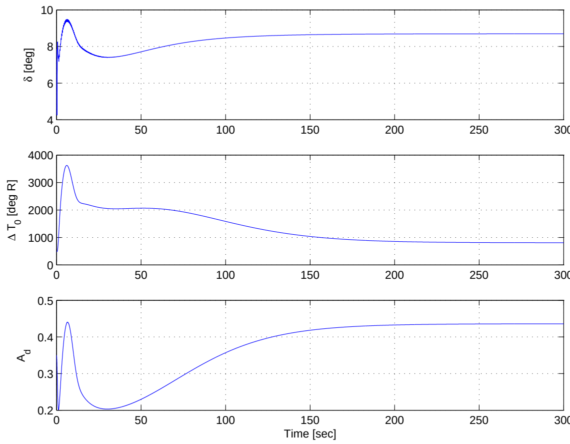

(b) Inputs with no Input Constraints

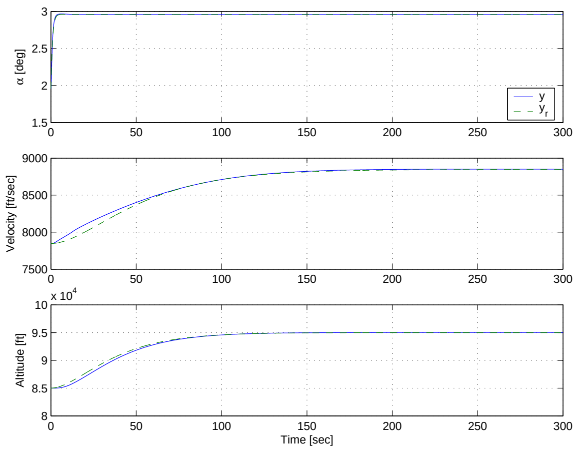

(c) Outputs with Input Constraints

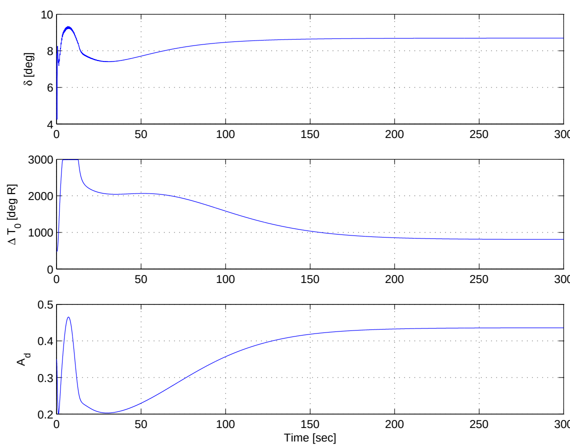

(d) Inputs with Input Constraints

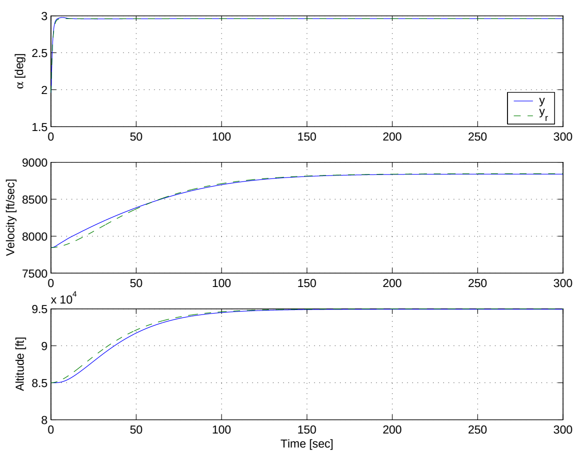

(e) Outputs with Anti-windup Control

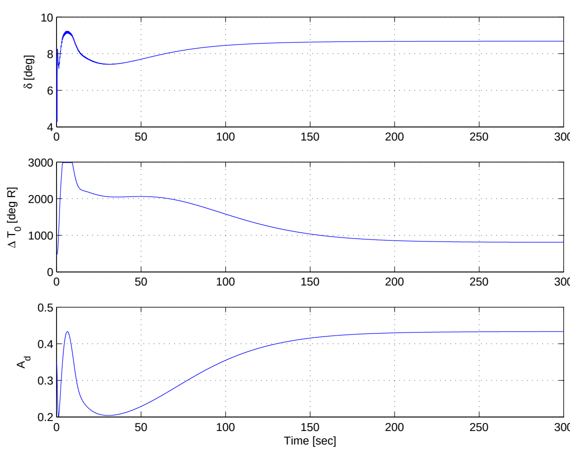

(f) Inputs with Anti-windup Control

Figure 5. Case 1: Nonlinear System Response

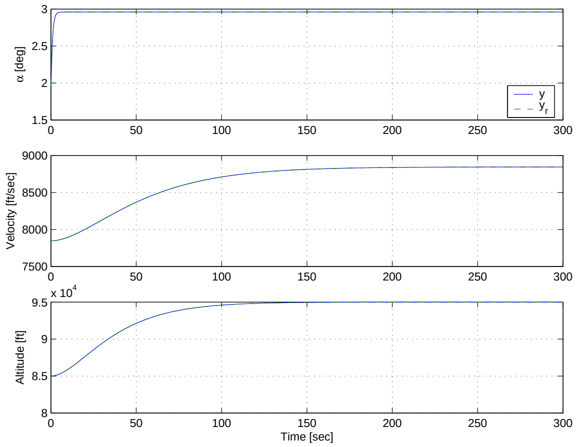

(a) Outputs with no Input Constraints

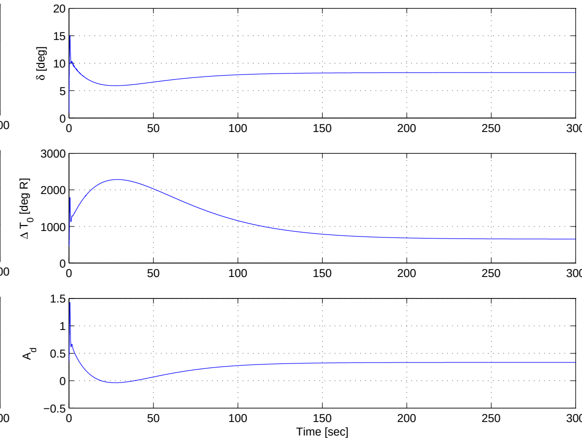

(b) Inputs with no Input Constraints

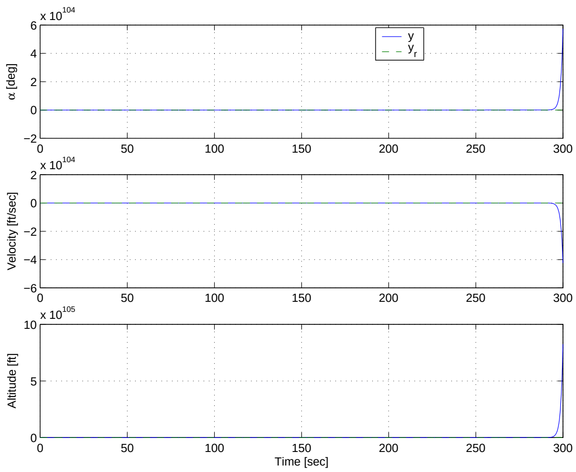

(c) Outputs with Input Constraints

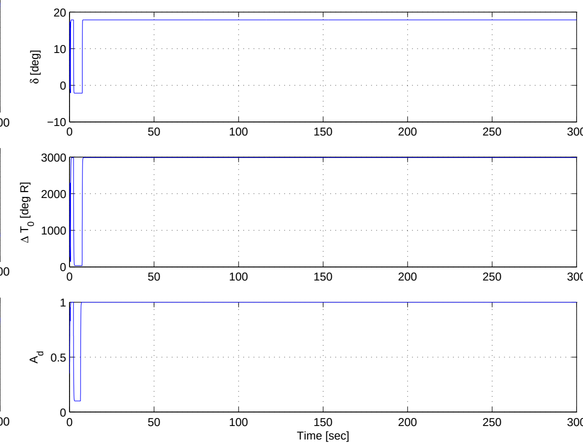

(d) Inputs with Input Constraints

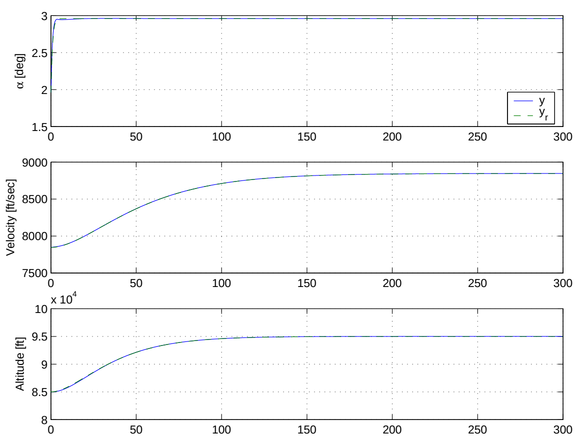

(e) Outputs with Anti-windup Control

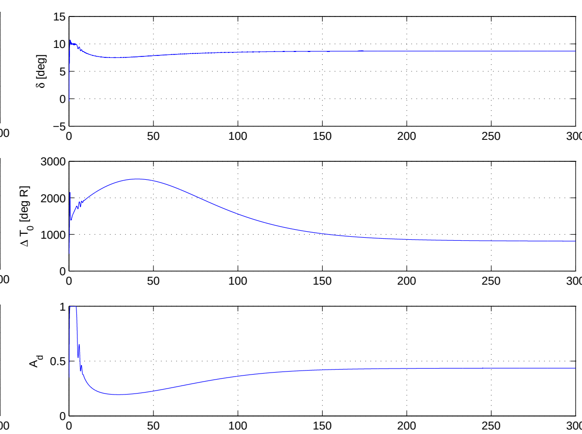

(f) Inputs with Anti-windup Control

Figure 6. Case 2: Linearized System Response with and without Input Constraints; Nonlinear System Response with Anti-windup Control

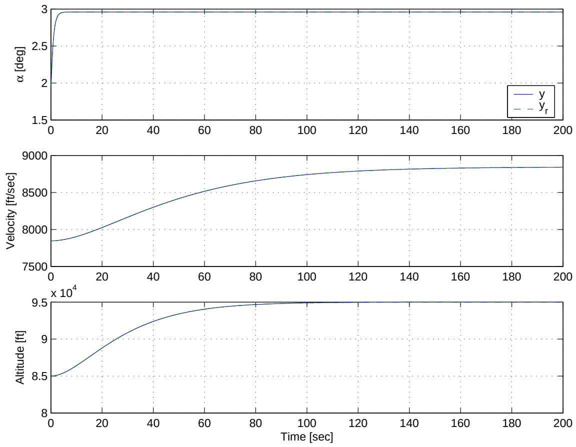

(a) Outputs with no Input Constraints

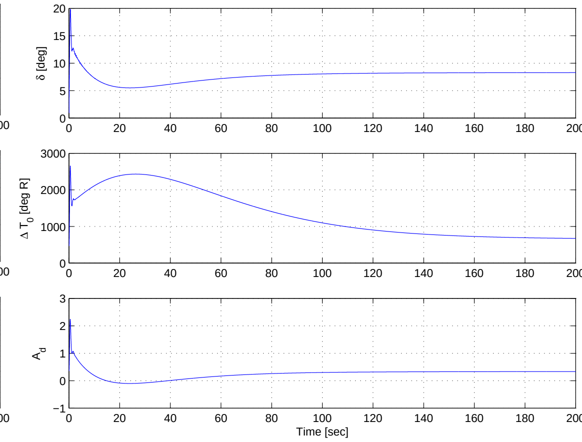

(b) Inputs with no Input Constraints

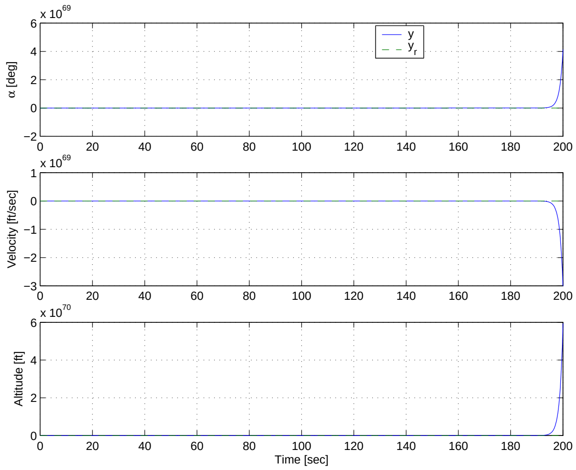

(c) Outputs with Input Constraints

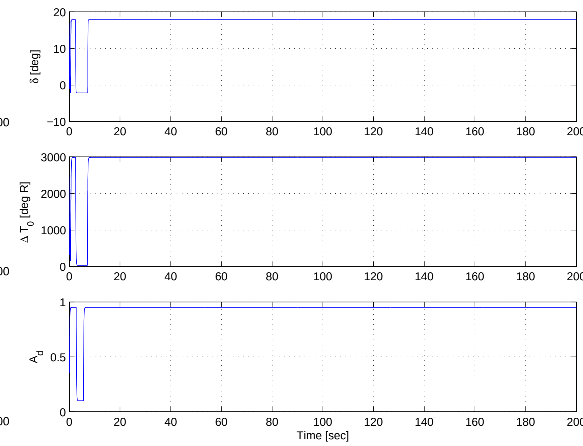

(d) Inputs with Input Constraints

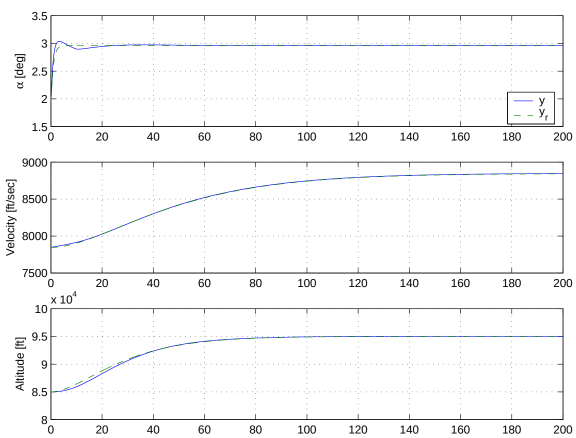

(e) Outputs with $Q_+ = 1$

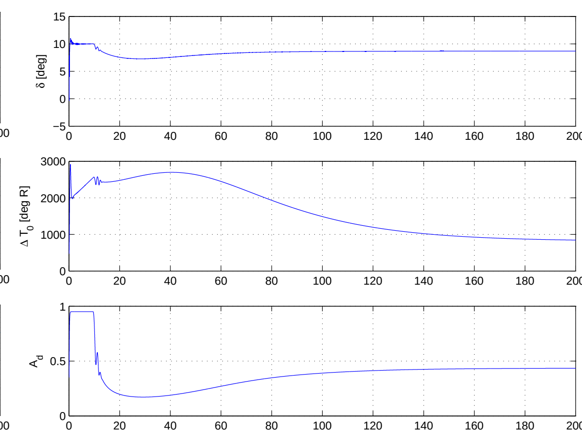

(f) Inputs with $Q_+ = 1$

Figure 7. Case 3: Linearized System Response with and without Input Constraints; Nonlinear System Response with Anti-windup Control